Review Article

Water-Solubilization of P(V) and Sb(V) Porphyrins and Their Photobiological Application

Jin Matsumoto,[1] Tsutomu Shiragami,[1] Kazutaka Hirakawa,[2] and Masahide Yasuda[1]

[1]*Department of Applied Chemistry, Faculty of Engineering, University of Miyazaki, Gakuen-Kibanadai, Miyazaki 889-2192, Japan*
[2]*Department of Applied Chemistry and Biochemical Engineering, Graduate School of Engineering, Shizuoka University,*
 Johoku 3-5-1, Hamamatsu, Shizuoka 432-8561, Japan

Correspondence should be addressed to Jin Matsumoto; jmatsu@cc.miyazaki-u.ac.jp
and Kazutaka Hirakawa; tkhirak@ipc.shizuoka.ac.jp

Porphyrins have been widely utilized as biochemical and biological functional chromophores which can operate under visible-light irradiation. Water-soluble porphyrins have been used as the drug for photodynamic therapy (PDT) and photodynamic inactivation (PDI). Although usual water-solubilization of porphyrins has been achieved by an introduction of an ionic group such as ammonium, pyridinium, sulfonate, phosphonium, or carboxyl to porphyrin ring, we proposed the preparation of water-soluble P and Sb porphyrins by modification of axial ligands. Alkyl (type A), ethylenedioxy (type E), pyridinium (type P), and glucosyl groups (type G) were introduced to axial ligands of Sb and P porphyrins to achieve water-solubilization of Sb porphyrin and P porphyrins. Here, we review their water-soluble P and Sb porphyrins from the standpoints of preparation, bioaffinity, and photosensitized inactivation.
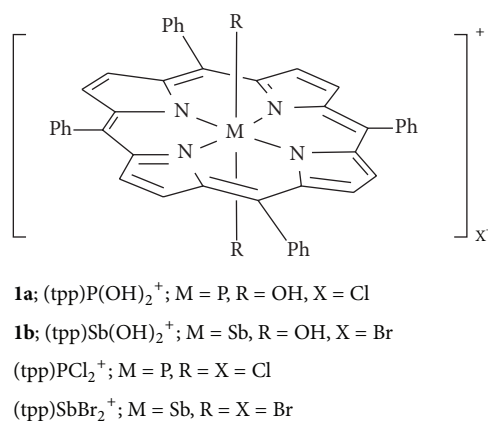
1. Introduction

Porphyrin complexes with high absorptivity in visible-light regions have been widely utilized as chemical and biological functional chromophores [1]. Porphyrin complexes are capable of versatile catalytic reactions through electron transfer or energy transfer under visible-light irradiation. Recently bioactive porphyrins have received much attention in connection with photoinactivation [2, 3] and photodynamic therapy (PDT) [4–7]. In general, the porphyrin compound tends to form face-to-face aggregates, resulting in less solubility even in organic solvents. For the biological application of porphyrins, water solubility is an important characteristic in handling the porphyrins in aqueous solution. Usual water-solubilization of metalloporphyrins is achieved by the modification of porphyrin ring by an ionic group such as ammonium [8], pyridinium [9–13], sulfonate [14–16], phosphonium [13, 17], or aminocarboxylate [18]. However, the preparation of these complexes is not so easy. Recently we have developed water-solubilization of P and Sb porphyrins by modification of axial ligands [19–26]. Tetraphenylporphyrin (H_2tpp) is a typical and commercially available porphyrin and can easily be converted to the P(V) and Sb(V) complexes. The P and Sb porphyrins are able to connect covalently with axial ligands through oxygen and nitrogen atoms, resulting in the highly stabilized complexes. Therefore the axial-ligand modified P and Sb porphyrins can conveniently provide a variety of water-soluble porphyrins with bioactivity and bioaffinity as well as high electron accepting ability. Here, we review water-soluble P and Sb porphyrins from the standpoints of preparation, bioaffinity, and photosensitization.

2. Water-Solubilization of Porphyrins

2.1. By Modification of Axial Ligands. It is believed that $(tpp)P(OH)_2{}^+$ (**1a**) $(tpp)Sb(OH)_2{}^+$ (**1b**) and $(tpp)Sb(OMe)OH^+$ (**2a**) are water-soluble since they are cationic compounds with hydrophilic hydroxogroup (Scheme 1). However, their water solubilities (C_W/mM), which were defined as saturated concentration in water, were still low. Therefore, the C_W of Sb porphyrins was enhanced

1a; (tpp)P(OH)$_2{}^+$; M = P, R = OH, X = Cl

1b; (tpp)Sb(OH)$_2{}^+$; M = Sb, R = OH, X = Br

(tpp)PCl$_2{}^+$; M = P, R = X = Cl

(tpp)SbBr$_2{}^+$; M = Sb, R = X = Br

SCHEME 1

FIGURE 1: Dependence of water solubility (C_W) of **2a**–**2g** on carbon number (n) of axial alkyl ligands. Plausible structure of aggregation of **2** in aqueous solution was shown in inset.

by an introduction of a variety of axial ligands. Modification of axial ligands of P and Sb porphyrins has been easily performed by alkylation of **1a** and **1b** with alkyl halides as well as ligand exchange of (tpp)PCl$_2{}^+$ and (tpp)SbBr$_2{}^+$ with alcohols. Matsumoto et al. and Yasuda et al. have modified axial ligands by alkyl (named as type A), ethylenedioxy (type E), N-alkyl pyridyl (type P), and glucosyl groups (type G) to provide water-soluble Sb porphyrin (**2**) [19–21] and P porphyrins (**3–5**) [22–25]. Table 1 lists the C_W of P and Sb porphyrins as well as spectroscopic data. Also, oil-solubility (C_O/mM) which was defined as solubility in 1,4-dioxane is listed in Table 1.

Type A of porphyrins (**2a**–**2g**, Scheme 2) was prepared by the ligand exchange of (tpp)Sb(OMe)Br$^+$Br$^-$ with alcohols. Introduction of axial alkyloxo ligands enhanced the C_W values of **2c**–**2g** [19–21]. For example, C_W (1.09 mM) of hexyloxo(methoxo)tetraphenylporphyrinatoantimony (**2c**) was much higher than that of the parent **2a** (C_W = 0.10 mM). As increase of carbon number (n) of axial alkyl ligands, the C_W of **2** increased until C_W reached 2.40 mM at n = 14, as shown in Figure 1. It was thought that hydrophobic alkyl ligand induced the formation of micelle type of aggregation. Therefore, the structure of **1** in aqueous solution was examined by the dependence of half-width of bands in the absorption spectra [12] and surface tension on the concentration of **2** in range from 1 μM to 100 μM. It was estimated that **2c**–**2g** with the larger C_W than 1 mM were present as aggregates in a concentration higher than 10 μM. In the NMR analysis in D$_2$O, the anisotropic higher field shifts compared with the NMR spectra in CD$_3$OD were observed at terminal methyl group on axial alkyl ligand. It was deduced that the alkyloxo ligands of **2c**–**2g** were arranged alternately in the aggregates, as illustrated in Figure 1 (inset). The long alkyl axial ligands with $n \geq 6$ were requisite for the high solubility in water. The diameter of the aggregates of **2c**–**2g** in water was determined to be around 100 nm by the dynamic light scattering method.

P porphyrins with two symmetric axial ligands in upper and lower positions can be easily synthesized while it is difficult to introduce ligands unsymmetrically to axial position. The introduction of two axial hexyloxo ligands did not enhance the C_W: that is, C_W of **3i** was still low
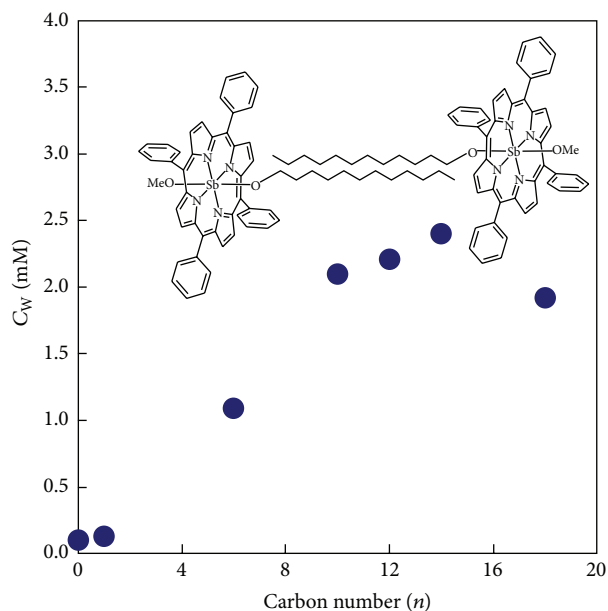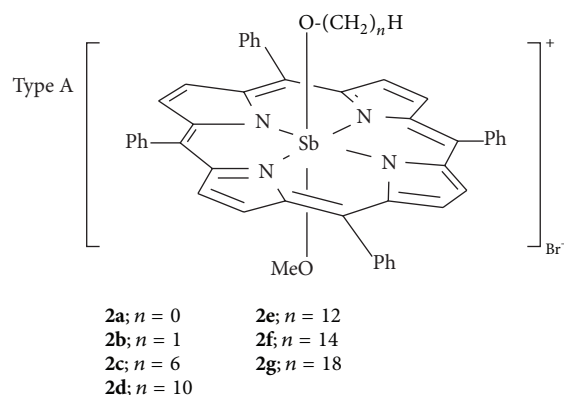
(0.023 mM). Therefore, hydrophilic ethylenedioxy group (–CH$_2$CH$_2$O–) was incorporated into the axial ligands in order to enhance C_W [22]. Bis(polyoxoalkyloxo)(tetraphenylporpyrinato)phosphorus (**3a**–**3k**, Scheme 3) was prepared by the reaction of polyoxa-alcohols (H(CH$_2$)$_n$(OCH$_2$CH$_2$)$_m$OH) with (tpp)PCl$_2{}^+$ in MeCN in the presence of a small amount of pyridine. The introduction of ethylenedioxy group improved C_W. For example, the C_W of **3h** (1.11 mM) became relatively higher compared with **3i** without the ethylenedioxy group. As the carbon number (n) of the alkyl group on H(CH$_2$)$_n$(OCH$_2$CH$_2$)$_2$– ligands decreased, the C_W values increased: C_W = 2.07 (n = 6; **3g**), 5.38 (n = 4; **3e**), 13.0 (n = 2; **3d**), and 13.9 mM (n = 1; **3c**) at m = 2. The maximum C_W was observed at **3b** (m = 3, n = 1), whose C_W was 17.4 mM. Thus, the C_W could be varied from 0.02 to 17.4 mM by the adjustment of m and n. The bioaffinity and photoinactivation of **2** and **3** to *Saccharomyces cerevisiae* (yeast) will be discussed in Sections 3.1 and 4.3.

The tricationic P porphyrins (**4a**–**4c**, Scheme 4) were prepared by the reactions of 3-alkylpyridine with bis(5-bromo-3-oxapentyloxo)tetraphenylporphyrinato-phosphorus(V) chloride, which was prepared by the reaction of **1a** with di(2-bromoethyl) ether [24]. Another type of tricationic P porphyrins (**4d**–**4f**) was prepared by N-alkylation of bis[3-(4-pyridyl)propoxo]tetraphenylporphyrinatophosphorus(V), which was prepared by the reaction of (tpp)PCl$_2{}^+$ with 3-(4-pyridyl)-1-propanol. The **4a**–**4c** containing both N-alkyl-pyridinio and ethylenedioxy units had large C_W (>63 mM) whereas **4d**–**4f** containing only N-alkylpyridinio group had >3 mM of C_W. It is well known that porphyrins tend to aggregate in aqueous solution to cause broadening of the absorption spectra. Therefore, we checked whether **4a**–**4f** aggregated or not in aqueous solution
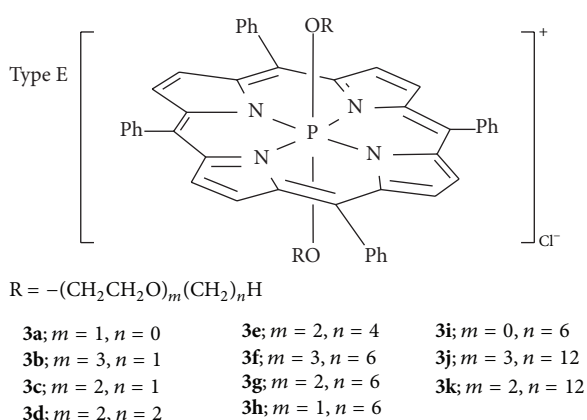
TABLE 1: Characterization of water-soluble porphyrins (**1–7**).

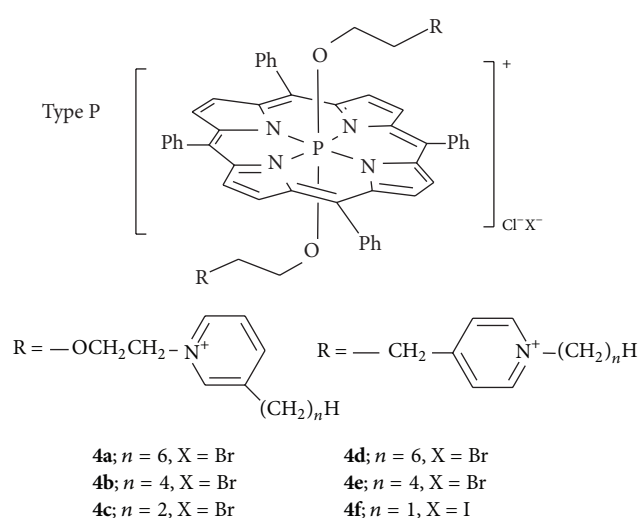| Type	Number	M	m, n, R	MW^a	$\varepsilon_Q/10^4\ M^{-1}cm^{-1}\ (\lambda_{max}/nm)^b$	$\Phi_\Delta\ (\tau_T/\mu s)^c$	$C_O/\mu M^d$	C_W/mM^d	$[P]_{ad}/mM$	$A_F/\mu M^{-1}h^{-1}$	Reference
Type A	**2a**	Sb	$n=0$	862.4	1.95 (551)	—	41	0.10	11.4	2.6	[21]
	2b	Sb	$n=1$	876.5	1.86 (550)	0.65	25	0.13	33.2	5.2	[21]
	2c	Sb	$n=6$	946.5	1.16 (550)	—	149	1.09	54.2	78.2	[21]
	2d	Sb	$n=10$	1002.7	1.59 (553)	0.53	139	2.10	49.8	45.3	[21]
	2e	Sb	$n=12$	1030.4	1.32 (553)	—	156	2.21	22.5	109.4	[21]
	2f	Sb	$n=14$	1058.4	1.24 (553)	—	66	2.40	nd	no	[21]
	2g	Sb	$n=18$	1114.9	1.42 (554)	—	—	1.92	—	—	[21]
Type E	**3a**	P	$m=1, n=0$	801.3	0.97 (559)	—	6090	10.4	7.3	—	[27]
	3b	P	$m=3, n=1$	1005.5	1.35 (560)	—	245	17.4	nd	5.2	[21]
	3c	P	$m=2, n=1$	917.4	1.40 (560)	0.62 (1.5)	140	13.9	22.6	2.5	[21]
	3d	P	$m=2, n=2$	945.5	1.44 (560)	0.69 (1.5)	169	13.0	25.0	9.7	[21]
	3e	P	$m=2, n=4$	1001.6	1.44 (560)	0.73 (1.6)	293	5.38	81.6	21.9	[21]
	3f	P	$m=3, n=6$	1145.8	1.39 (559)	—	415	14.4	123	—	[21]
	3g	P	$m=2, n=6$	1057.7	1.37 (561)	—	244	2.07	161	188.7	[21]
	3h	P	$m=1, n=6$	969.6	1.01 (560)	—	242	1.11	171	174.6	[21]
	3i	P	$m=0, n=6$	881.5	1.41 (560)	—	178	0.02	—	—	[23]
	3j	P	$m=3, n=12$	1314.1	1.42 (561)	—	440	14.5	nd	—	[21]
	3k	P	$m=2, n=12$	1226.0	1.39 (560)	—	242	0.26	nd	—	[21]
Type P	**4a**	P	$n=6$	1341.7	1.22 (560)	[4.91]	284	63.6	nd	2.1	[24]
	4b	P	$n=4$	1285.5	1.29 (560)	—	245	112	nd	4.5	[24]
	4c	P	$n=2$	1229.5	1.40 (560)	[4.82]	2	>120	nd	7.2	[24]
	4d	P	$n=6$	1281.6	1.45 (560)	—	149	5.84	nd	no	[24]
	4e	P	$n=4$	1225.5	1.18 (560)	—	500	6.10	nd	no	[24]
	4f	P	$n=1$	1235.4	1.38 (560)	—	0	3.35	9.2	no	[24]
Type G	**5a**	P		1373.8	1.35 (559)	[5.6]	>25000	131	—	—	—^e
	5b	P		1037.5	1.30 (559)	[5.6]	6830	>150	—	—	—^e
Others	**1b**	Sb		848.4	2.14 (550)	0.48	—	0.08	—	—	[2]
	6a	P	$n=4$	862.8	1.31 (560)	—	—	5.0	—	—	—^e
	6b	P	$n=6$	834.8	1.19 (560)	—	—	60.0	—	—	—^e
	6c	P	$n=6$	1183.2	1.23 (561)	—	—	80.0	—	—	—^e
	6d	P	$n=10$	1127.1	0.96 (561)	—	—	45.0	—	—	—^e
	7a	P	$R=CH_3$	741.2	1.02 (560)	—	8000	0.31	—	—	[28]
	7b	P	$R=CH_2CH_3$	769.3							[28]
	7c	P	$R=CH_2CF_3$	877.2							[28]

[a] Molecular weight.
[b] Molar absorption coefficient (ε_Q) of Q-band in an aqueous solution. The values in parenthesis were the absorption maxima of the Q-band.
[c] Quantum yields (Φ_Δ) for the formation of $^1O_2$ in an H_2O solution. The values in parenthesis were lifetime (τ_T) in μs of triplet state of **3c**-**3d**. The values in bracket were fluorescence lifetime (τ_S) in ns from excited singlet state.
[d] C_W and C_O were solubility in water and 1,4-dioxane, respectively.
[e] Unpublished results.

Type A

O-(CH$_2$)$_n$H

Ph

N   N

Ph   Sb   Ph

N   N

MeO   Ph

Br$^-$

2a; $n = 0$ **2e**; $n = 12$
2b; $n = 1$ **2f**; $n = 14$
2c; $n = 6$ **2g**; $n = 18$
2d; $n = 10$

Scheme 2: Type A: alkyloxo(methoxo)antimonytetraphenylporphyrins (**2**).

Type E

Ph   OR

N   N

Ph   P   Ph

N   N

RO   Ph

Cl$^-$

R = −(CH$_2$CH$_2$O)$_m$(CH$_2$)$_n$H

3a; $m = 1, n = 0$ **3e**; $m = 2, n = 4$ **3i**; $m = 0, n = 6$
3b; $m = 3, n = 1$ **3f**; $m = 3, n = 6$ **3j**; $m = 3, n = 12$
3c; $m = 2, n = 1$ **3g**; $m = 2, n = 6$ **3k**; $m = 2, n = 12$
3d; $m = 2, n = 2$ **3h**; $m = 1, n = 6$

Scheme 3: Type E: bis(polyoxoalkyloxo)(tetraphenylporpyrinato) phosphorus (**3**).

Type P

O   R

Ph

N   N

Ph   P   Ph

N   N

R   O   Ph

Cl$^-$X$^-$

R = —OCH$_2$CH$_2$—N$^+$ (CH$_2$)$_n$H   R = — CH$_2$—N$^+$—(CH$_2$)$_n$H

4a; $n = 6$, X = Br   **4d**; $n = 6$, X = Br
4b; $n = 4$, X = Br   **4e**; $n = 4$, X = Br
4c; $n = 2$, X = Br   **4f**; $n = 1$, X = I

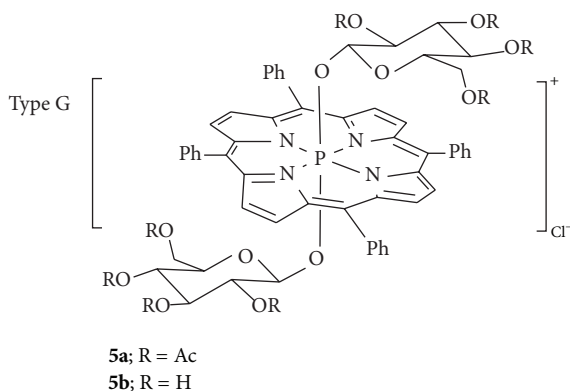Scheme 4: Type P: pyridinio-bonded tricationic phosphorus-porphyrins (**4**).

by absorption spectra. We have previously reported that half-width (HW) of Soret band of P porphyrins was about 16 nm in the case of monomer form whereas HW became more than 20 nm when P porphyrins formed aggregates [22]. The absorption spectra of **4a**–**4f** showed Soret band with 16.6–18.2 nm of HW, showing no aggregation even in phosphate buffer solution.

Koenigs-Knorr synthesis is a glycosylation method of alcohols in the presence of soft Lewis acids such as silver carbonate which plays a role to activate glycosyl halides. For the glycosylation of **1a** which had chloride ion, we modified Koenigs-Knorr synthesis. Tetra-*O*-acetyl-5-bromo-α-D-glucopyranose was firstly activated with Ag$_2$CO$_3$ in the presence of molecular sieves in MeCN and then subjected to glycosylation of **1a** P porphyrin which was stereoselectively introduced at β-position of glucose. This modification provided **5a** in 44% yield (Scheme 5). The deacetylation of **5a** was quantitatively transformed to **5b** by Zemplen reaction which was carried out in MeOH with a catalytic amount of NaOMe [25]. The C_W of **5a** was determined to be 131 mM, as listed in Table 1. The C_W of **5b** was too large to determine precisely (>150 mM). Moreover, solubility of **5b** in physiological saline was maintained at 6.2 mM, enough to handle it in biological systems. The C_W values are listed in Table 1.
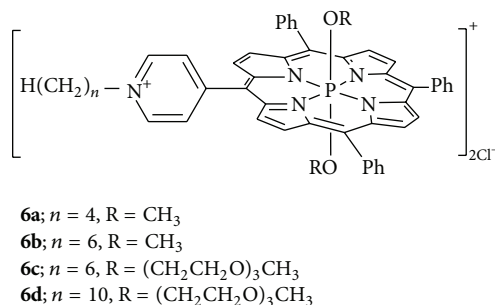
2.2. By Modification of Porphyrin Rings.

As has been reviewed by Kalyanasundaram [26], the modification of porphyrin ring by hydrophilic *N*-methylpyridiniumyl groups is the most popular method for water-solubilization of porphyrins. Water-soluble metalloporphyrins (metal = Zn [29, 30], Fe [31], Mn [32], Cu [33], Co [34], and Au [35]) containing *N*-methylpyridiniumyl group have been reported. Also, we prepared P porphyrin containing *N*-alkyl pyridyl group on the porphyrin (**6a**–**6d**, Scheme 6). The C_W values of **6b**–**6d** were large (>45 mM) as listed in Table 1.

3. Bioaffinity of Porphyrins

Bioaffinity of porphyrins can be conveniently evaluated using microorganisms such as *S. cerevisiae* and *Escherichia coli* and specific proteins such as human serum albumin (HSA) and concanavalin A (ConA) acting as drug delivery proteins and a glucose-binding protein, respectively. In particular *S. cerevisiae* is a large size microorganism whose diameter is 5 μm and can survive in not only buffer solution but also

Scheme 5: Type G: di(glycosyl)(tetraphenylporpyrinato)-phosphorus (**5**).

5a; R = Ac
5b; R = H

6a; $n = 4$, R = CH$_3$
6b; $n = 6$, R = CH$_3$
6c; $n = 6$, R = (CH$_2$CH$_2$O)$_3$CH$_3$
6d; $n = 10$, R = (CH$_2$CH$_2$O)$_3$CH$_3$

Scheme 6

Figure 2: Dependence of [P]$_{ad}$ on n. **2** (●) and **3** (○).

pure water. Therefore, it is easy to handle in sterilization experiments and quantitative analysis.

3.1. Bioaffinity of 2 and 3 toward S. cerevisiae. Bioaffinity of complexes **2** and **3** towards *S. cerevisiae* cells was examined. The amounts of **2** and **3** incorporated into yeast cells were determined by quantitative analysis using a confocal laser scanning microscope (CLSM) as follows [21, 23]. An aqueous solution of **2** and **3** (0.5 mL, 50 μM) was added to the cell suspension (1.0 mL; ca. 2.5×10^4 cell mL^{-1}) of *S. cerevisiae*. However it is difficult to perform CLSM analysis since cells moved around by their Brownian motion. Therefore, an aqueous solution of agar (1 wt%; 1.0 mL) was added to the solution in order to stop the motion of cells during the CLSM analysis. A portion of the prepared aqueous solution containing **2** and **3** (10 μM), *S. cerevisiae* (ca. 1.0×10^4 cell mL^{-1}), and agar (0.4 wt%) was taken on a space (1 cm $\times$ 1 cm) surrounded by silicone spacer (thickness 50 μm) put on a glass slide. The glass slide was set on the stage to be subjected to absorption spectrophotometry with the CLSM. The saturated adsorption concentrations ([P]$_{ad}$) of porphyrins (**2** and **3**) on yeast were determined by absorption spectrophotometry at the Q-band using molar coefficiency (Table 1), path length (b), and absorbance (A) according to Lambert-Beer's law: $A = \varepsilon b$[P]$_{ad}$. The b was determined by the CLSM fluorescence image where the fluorescence was
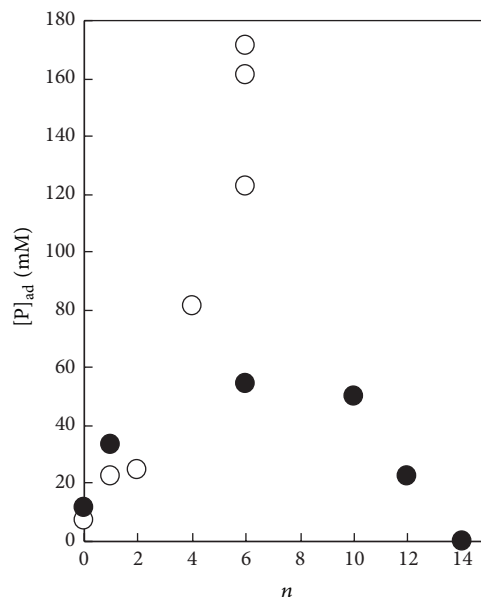
emitted from the inside rather than the walls of cells. The observed [P]$_{ad}$ values are summarized in Table 1.

Figure 2 shows the dependence of [P]$_{ad}$ on carbon number (n) of the alkyl group on axial ligands of **1** and **2**. In the cases of **2a**–**2f**, [P]$_{ad}$ values depended on n. The [P]$_{ad}$ values reached maximum at $n = 6$ (**2c**). When $n = 14$ (**2f**), the [P]$_{ad}$ was less than a measurable lower limit (<1.65 mM). Thus bioaffinity of **2** and **3** to yeast can be evaluated by [P]$_{ad}$ value. Also, in the cases of **3a**–**3f**, the [P]$_{ad}$ values depended on n, as shown in Figure 2. The [P]$_{ad}$ values reached the maximum at $n = 6$ (**3h**). The **3h** was concentrated into 171 mM in *S. cerevisiae* at 17100-fold from 10 μM of an aqueous solution. However, when $n = 12$, the [P]$_{ad}$ decreased to be less than a measurable lower limit. Thus n was optimized to be 6. Photosensitized inactivation of *S. cerevisiae* using **2** and **3** will be described in Section 4.3.

Moreover, adsorption mechanism of **3** in cells was discussed by the concentration-dependence aggregation in aqueous solution [20]. The structure of **3** in aqueous solution of the concentration range from aqueous 1 μM to 1.0 mM was estimated by measuring surface tension, absorption spectra, and NMR spectra. As results, it was found that the **3e**–**3h** ($n = 4$ and 6) were solved as monomers below 10 μM and formed aggregates above a range of 10–50 μM (Scheme 7(b)). This showed that the **3e**–**3h** with a high [P]$_{ad}$ of 123–171 mM could pass through the cell wall to accumulate inside the cell. Once inside the cell, where they reached a concentration of more than 10 μM, they formed aggregates that were unable to escape to the outside of the cell. We called this the *ship-in-a-bottle effect*. On the other hand, the **3b**–**3d** did not form aggregates at any concentrations in the range from 1 μM to 1 mM. This indicated that they easily passed through the cell wall in both directions (Scheme 7(a)). Therefore, [P]$_{ad}$ values remained <25 mM. In the case of **3i**–**3j**, whose [P]$_{ad}$ values were very low, passage through the cell wall was not possible
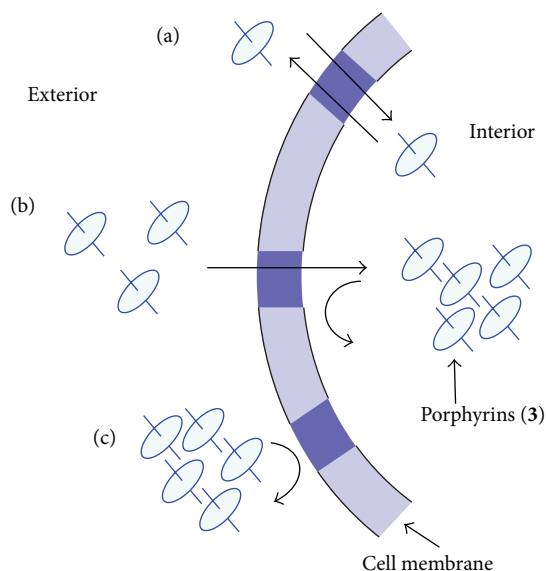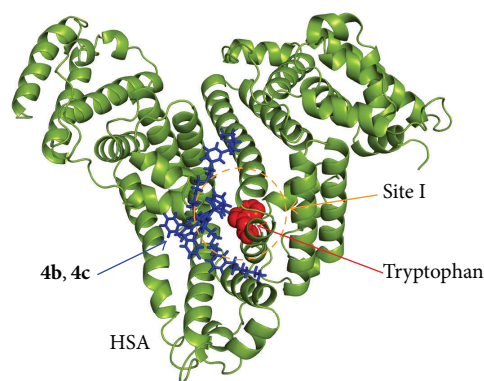
SCHEME 7: Relationship between aggregation of **3** and its accumulation in a cell. The aggregation behaviors of **3** were classified into following three types: (a) **3b**–**3d** which did not form aggregates at any concentration, (b) **3e**–**3h** which formed aggregates at a concentration higher than 10 or 20 μM, and (c) **3i-3j** which form aggregation at any concentration <1 mM. The *ship-in-a-bottle effect* appeared in the case of (b).
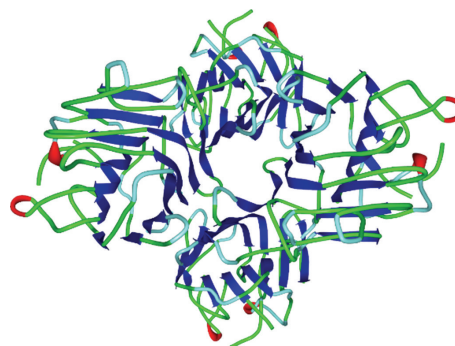

SCHEME 8: Binding of **4b**-**4c** on Site I of HAS.

SCHEME 9: Structure of concanavalin A (ConA). The glucose-binding sites are shown in red color.

because aggregates formed even at <1 μM (Scheme 7(c)). Although the adsorption of P porphyrins (**4**) into *S. cerevisiae* was examined in a similar manner as **2** and **3**, the adsorption of **4** into *S. cerevisiae* was not observed.

3.2. Bioaffinity of 4 toward HSA. HSA (MW 66500) which is the most abundant plasma protein has the ability to bind many kinds of drugs and is applied to drug delivery systems [36] (Scheme 8). Therefore, interaction between P porphyrins (**4**) and HSA was examined by the fluorescence quenching of HSA by **4** (Method A) as well as spectral changes in absorption (Method B) and fluorescence (Method C) spectra of **4** by the addition of HSA [24].

Analysis by Methods A and B showed that the adsorption obeyed Langmuir-type adsorption with binding constants (K): log K = 6.3 (**4a**), 4.3 (**4b**), 4.1 (**4c**), 4.6 (**4d**), 4.7 (**4e**), and 5.1 (**4f**). HSA has one tryptophan residue on major drug-biding site (Site I) [37]. The ratio of the number of molecules of **4** adsorbed on Site I to the total number of molecules of **4** adsorbed on whole HSA, which was defined as f values, can be analyzed by Method C using modified Stern-Volmer plots [38]. By the analysis of Method C, compounds **4** were classified into three categories according to their f values: 1, 0.6, and 0.2. The **4b** (n = 4) and **4c** (n = 2) with f values of 1.0 bind to Site I site-specifically (Scheme 8). However, **4a** (n = 6), **4d** (n = 6), and **4e** (n = 4) with f values of 0.6 bind to HSA at two types of sites with similar affinities. In the case of **4f** (n = 1) with an f value of 0.2, most molecules of **4f** adsorbed on the HSA far from the tryptophan residue leading to inefficient quenching. Thus,

the length of the alkyl chain affects the site-specific binding to HSA. When **4** had moderately long alkyl chains on the pyridinio group, **4** was adsorbed strongly on the hydrophobic pocket near a tryptophan residue of HSA.

3.3. Bioaffinity of 5 toward Concanavalin A. ConA (MW 25700 for one subunit) is a glucose-binding protein which is composed of four identical subunits under basic conditions (pH > 7) [39]. Each subunit has one sugar-binding site which includes two tyrosine residues (tyrosine-12 and tyrosine-100) [40, 41] (Scheme 9). Moreover, ConA emitted fluorescence at 335 nm under excitation at 230 nm, since the subunit contains four tryptophan and seven tyrosine residues which have absorption at UV region. There are tyrosine-12 and tyrosine-100 at the sugar-binding site and they are able to interact with sugar moieties [41, 42]. However, four tryptophan residues do not exist near the sugar-binding site.

According to Methods A, B, and C which have been reported for the interaction of **4** with HSA, the interaction of ConA with **5** was analyzed. Analysis by Method A showed that **5a** and **5b** strongly bound ConA near to tryptophan and/or tyrosine residues. Analysis by Method B provided 4.5 × 10^4 and 6.4 × 10^4 M^{-1} of the binding constants (K) for **5a** and **5b**, respectively.

Fluorescence spectral changes of **5** with L-tryptophan and L-tyrosine were examined in the buffer solutions. L-tryptophan quenched the fluorescence of **5**, whereas L-tyrosine did not quench. Free energy change (ΔG) for an electron transfer from L-tryptophan to the excited singlet state of **5** (**5***) was assumed according the Rehm-Weller equation: $\Delta G = E_{1/2}{}^{ox} - E_{1/2}{}^{red} - E^{0-0}$, where $E_{1/2}{}^{ox}$ denotes an oxidation potential of L-tryptophan (0.638 V versus Ag/Ag$^+$), $E_{1/2}{}^{red}$ denotes a reduction potential of **5a** (–0.895 V) and **5b** (–0.835 V), and E^{0-0} denotes excitation energies of **5a** and **5b** which were 2.02 eV (612 nm) and 2.03 eV (614 nm), respectively. Thus, the ΔG values for electron transfer from L-tryptophan to **5*** were estimated as negative values for **5a** (–0.547 eV) and **5b** (–0.497). Therefore, the fluorescence quenching of **5** with ConA might proceed through the photoinduced electron transfer from tryptophan residues to **5*** whose fluorescence lifetimes were determined to be 5.6 ns in aqueous solution. Actually, the fluorescence of **5a** was quenched with ConA whereas the fluorescence of **5b** was not quenched with ConA (Method C). The **5a** adsorbed near these tryptophan residues without site-specificities. The **5b** adsorbed at the site near tyrosine residues but far from tryptophan residues.

4. Photosensitization of Porphyrins

4.1. Mechanism of Photosensitization.

The photosensitization by porphyrins mainly proceeds through two processes such as electron transfer from biomolecules to the photoexcited photosensitizer (Type I mechanism) and energy transfer from photoexcited photosensitizer to oxygen molecule to generate singlet oxygen ($^1O_2$) (Type II mechanism). The $^1O_2$ is a very important reactive oxygen species for the photosensitized reaction of porphyrins, because $^1O_2$ can be easily generated by a wide range of wavelengths (ultraviolet region ~ near-infrared region) including visible light. Formation of other reactive oxygen species, such as superoxide and hydroxyl radicals, in general, requires ultraviolet radiation. The electron transfer and $^1O_2$ generation processes lead to the oxidation of guanine residues of DNA and certain amino acid residues of protein.

4.2. Photosensitized DNA Damage by 1b and 1a.

DNA is an important targeting biomacromolecule of photosensitized reaction [42–44]. The **1b** demonstrates bactericidal activity during photoirradiation and this effect has been applied for water sterilization [45]. To elucidate the mechanism of phototoxic effect of **1b**, its photodamaging activity for biomacromolecule was investigated using DNA as a model targeting biomacromolecule. Photoirradiated **1b** damaged [^{32}P]-5$'$-end-labeled DNA fragments [46]. **1b** induced markedly severe photodamage to single-stranded DNA rather than to double-stranded DNA. Photoexcited **1b** frequently caused DNA cleavage at the guanine residues after $E.\ coli$ formamidopyrimidine-DNA glycosylase or piperidine treatment. These results indicated the formation of 8-oxo-7,8-dihydro-2$'$-deoxyguanine (8-oxo-G), a typical oxidized product of guanine. HPLC measurement also confirmed the
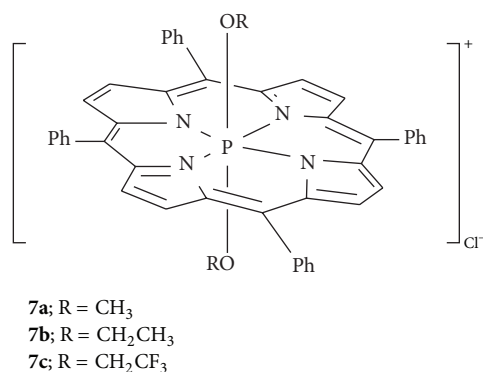
formation of 8-oxo-G and showed that the content of 8-oxo-G in single-stranded DNA is larger than that in double-stranded DNA. Because the single-stranded DNA can be easily oxidized by $^1O_2$, this result suggests the contribution of $^1O_2$-mediated oxidation of guanine. The effects of scavengers of reactive oxygen species on DNA damage also supported the involvement of $^1O_2$. These results have shown that the mechanism via $^1O_2$ formation mainly contributes to the phototoxicity of **1b**.

On the other hand, **1b** induced DNA damage specifically at the underlined G of 5$''$-G̲G, 5$''$-G̲GG, and 5$''$-G̲GGG in double-stranded DNA. The sequence-specificity of DNA damage is quite similar to that induced by the Type I photosensitizers [47]. The redox potential of one-electron oxidation of guanine is lowest in the four nucleobases [48]. Furthermore, the molecular orbital (MO) calculations have revealed that the consecutive guanines in double-stranded DNA significantly lower the highest occupied MO energy [49, 50]. Consequently, the consecutive guanines are selectively damaged through the electron transfer mechanism. These results showed that photoinduced electron transfer slightly participates in the photosensitized reaction of **1b**.

1b induces DNA photodamage via the generation of $^1O_2$ and electron transfer. Similar mechanisms can damage other biomacromolecules, such as protein and the phospholipid membrane. The damage to biomacromolecules via these mechanisms may participate in the phototoxic effect of **1b**.

The phosphorus(V) porphyrin also induces an oxidative electron transfer reaction [51]. The **1a**, a cationic water-soluble porphyrin, induced DNA photodamage via similar mechanism of **1b**, $^1O_2$ generation and electron transfer [51]. The study of near-infrared emission measurements demonstrated the $^1O_2$ generation by photoexcited **1a**. The fluorescence quenching of **1a** by DNA supported the electron transfer mechanism. Under aerobic conditions, **1a**-photosensitized damage was more severe for single-stranded DNA compared to its double-stranded counterpart. Photoirradiated **1a** damaged every guanine residue in single-stranded DNA. HPLC measurements confirmed the formation of 8-oxo-G. The guanine-specific DNA damage and the enhancement in single-stranded DNA suggest that the $^1O_2$ generation mainly contributes to the mechanism of DNA photodamage by **1a** similarly to that by **1b**. On the other hand, for double-stranded DNA, photosensitized damage at consecutive guanines was much less pronounced. Because the consecutive guanines act as a hole trap [47–50], this DNA-damaging pattern suggests the partial involvement of electron transfer mechanism. However, DNA damage by electron transfer mechanism was not a main mechanism, possibly due to the reverse electron transfer mechanism.

4.3. Photosensitized Protein Damage by 7.

Protein is also an important targeting biomacromolecule. The photosensitized protein damage by phosphorus(V) porphyrin has been investigated using the abovementioned HSA as a protein model [28]. A water-soluble porphyrin, dimethoxyP(V) tetraphenylporphyrin chloride (Scheme 10, **7a**), photosensitized HSA damage. The quantum yield of $^1O_2$ generation

7a; R = CH$_3$
7b; R = CH$_2$CH$_3$
7c; R = CH$_2$CF$_3$

SCHEME 10

—— Before irradiation
- - - After irradiation

FIGURE 3: Fluorescence spectra of the tryptophan residue of HSA. The sample solution containing HAS (10 μM) and **7a** (10 μM) in a sodium phosphate buffer (10 mM, pH 7.6) was irradiated for 30 min. Ex: 298 nm.

(Φ_Δ) by **7a** (0.64 in ethanol) was comparable with that of typical porphyrin photosensitizers. Absorption spectrum measurement demonstrated the binding interaction between **7a** and HSA. HSA has one tryptophan residue. Since tryptophan, a relatively strong fluorescent amino acid, is easily oxidized by both mechanisms (^{1}O$_2$ generation and electron transfer), leading to fluorescence quenching (Figure 3), the fluorometry of tryptophan is a convenient method to evaluate the protein damage. Photoirradiated **7a** damaged the amino acid residue of HSA, resulting in the decrease of the fluorescence intensity from the tryptophan residue of HSA. Sodium azide (NaN$_3$), a ^{1}O$_2$ quencher, partially inhibited the HSA damage, supporting the ^{1}O$_2$-mediated protein damage. However, the effect of sodium azide is not completed, suggesting that the electron transfer mechanism contributes to protein damage as does ^{1}O$_2$ generation. The decrease of the fluorescence lifetime of **7a** by HSA supported the electron transfer mechanism. The estimated contribution of the electron transfer mechanism is 0.64. These results suggest that the activity of **7a** can be preserved under lower oxygen concentration condition such as tumor.

The specific characteristics of the phosphorus(V) porphyrin are the variety of the substituted axial ligand and the relatively low redox potential of the one-electron reduction in the photoexcited state. The fluorination effect of the axial ligand of phosphorus(V) porphyrin (Scheme 10) on the photosensitized reaction has been examined [52]. As a target protein model, HSA was used. The activity of ^{1}O$_2$ generation by diethoxy (tetraphenylporphyrinato)phosphorus(V) complex (**7b**) was slightly improved by the fluorination of the ethoxy chains (**7c**). The quantum yields of ^{1}O$_2$ generation in sodium phosphate buffer were 0.59 and 0.68 for **7a** and **7b**, respectively. Absorption spectrum measurements demonstrated the binding interaction between these phosphorus(V) porphyrins and HSA. Photoirradiated phosphorus(V) porphyrins damaged the amino acid residue of HSA, resulting in the decrease of the fluorescence intensity from the tryptophan residue. A ^{1}O$_2$ quencher, NaN$_3$, could not completely inhibit the damage of HSA, suggesting that the electron transfer mechanism contributes to protein damage. The decrease of the fluorescence lifetime of these porphyrins by HSA supported the electron transfer mechanism. The estimated
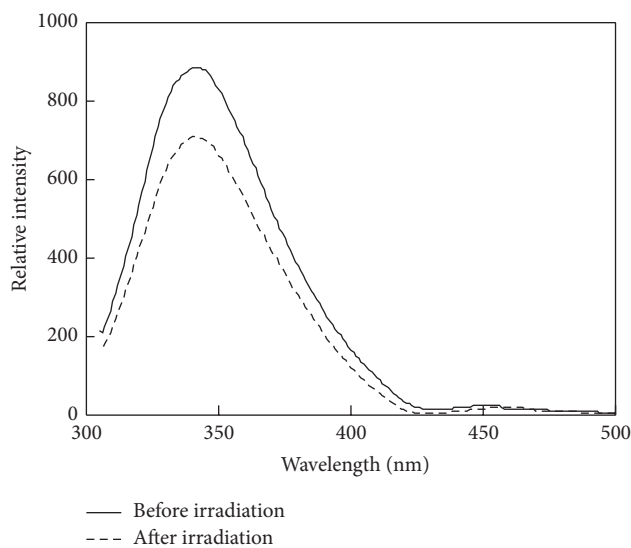
contributions of the electron transfer mechanism are 0.57 and 0.44 for the fluorinated and nonfluorinated P(V) porphyrins, respectively. The total quantum yield of the protein photooxidation was slightly enhanced by this axial fluorination.

4.4. Photosensitized Inactivation of S. cerevisiae by 2 and 3. In order to use **1a** and **1b** as photocatalyst in aqueous solution, these porphyrins were fixed on silica gel to produce the composite of porphyrins with silica gel. These composites were utilized for photochemical bactericidal reaction of *E. coli* [53], *S. cerevisiae* (yeast) [54], and *Legionella pneumophila* [45]. In particular, the composite was applied to the bactericidal reaction of *Legionella* species occurring in cooling tower and public fountain under irradiation of fluorescent lamp and sun light. Details have been published in review [2]. Here, we review the photosensitized inactivation of *S. cerevisiae* by water-soluble Sb and P porphyrins.

The photosensitized inactivation *S. cerevisiae* by Sb porphyrins (**2a–2f**) and P porphyrins (**3b–3h**) was examined. The photoinactivation under an argon-saturated atmosphere did not occur at all. Therefore, ^{1}O$_2$ was responsible for the active species of the photoinactivation. Under visible-light irradiation, **2** and **3** were excited to singlet state to transform to triplet state with high efficiency. The energy transfer from the triplet state of **2** and **3** to oxygen molecules in a ground state (^{3}O$_2$) took place to generate ^{1}O$_2$ through Type II mechanism. The values of Φ_Δ for these porphyrins were determined in an aqueous solution to be 0.48 (**1b**), 0.65 (**2b**), 0.53 (**2d**), 0.62 (**3c**), 0.69 (**3d**), and 0.73 (**3e**). These values were comparable values with other metalloporphyrins: 0.56 (H$_2$(tpp)), 0.65 (Zn(tpp)), and 0.62 (Mg(tpp)) [55]. The lifetimes of triplet state of **3b–3d** were estimated from the time profile of ^{1}O$_2$ emission and were determined to be 1.5–1.6 μs.

The photoinactivation of *S. cerevisiae* was performed for an aqueous solution (10 mL) of *S. cerevisiae* NBRC 2044 (1×10^4 cell mL^{-1}) and **2** and **3** (5–500 nM) in an L-type tube under irradiation by a fluorescent lamp on a reciprocal shaker. The photoinactivation was evaluated by the activity factor ($A_F/\mu M^{-1} h^{-1}$) which was derived by $A_F = ([P]_M \times T_{1/2})^{-1}$ using the minimum effective concentrations of **2** and **3** ($[P]_M/\mu M$) and half-life ($T_{1/2}/h$) which is the time required to be reduced to one-half initial concentration of *S. cerevisiae*. As listed in Table 1, the large A_F values (12.6–188.7 M^{-1} h^{-1}) were obtained in **2c**–**2e** and **3e** and **3g**-**3h** which have large $[P]_{ad}$ values (22.5–171 mM) and long alkyl chain ($n = 6$–12). It was requisite that **2** and **3** were both water-soluble and oil-soluble. Presumably the oil-soluble feature was advantageous in passing through the cell wall of the yeast which consisted of hydrophobic peptidoglycan and the water-soluble feature was advantageous in the adsorption occurring at hydrophilic sites inside the cell, causing fatal damage to the yeast.

4.5. Modeling of PDT Using a Phospholipid Liposome. As a model for PDT, the photosensitization of **2e** was investigated in a phospholipid liposome (LP) where target cell's substrate was modeled by 9,10-dimethylanthracene (DMA) [26]. The **2e** photosensitized the oxidation of DMA to 9,10-epidioxy-DMA (epidioxy-DMA) [56, 57] in LP. The LP was prepared by Banghom method [58] using 1,2-dipalmitoyl-*sn*-glycerol 3-phosphocholine (DPPC) (Scheme 11). A chloroform solution of DPPC (2.0 mM, 1.0 mL) was added to a 25 mL flask, and then CHCl$_3$ was removed with a rotary evaporator under reduced pressure at 40°C. All traces of the organic solvent were then removed by drying with a vacuum pump. The resulting thin film was hydrated with pure water in an ultrasonic bath at 70°C for 30 min to give an LP solution. The LP solution was cooled to room temperature and maintained at 25°C overnight. The LPs were found to have diameters of 50–240 nm (average diameter of 83 nm) by dynamic light scattering, measured at 25°C. DMA and **2e** were incorporated into LP as follows. Next, an aqueous solution of **2e** (0.1 mM, 6 μL) and a MeOH solution of DMA (1 mM, 2.7–15.0 μL) were added to an aqueous LP solution (3.0 mL, DPPC = 0.6 μmol) to give an LP solution (3.0 mL) containing **2e** (0.2 μM; 6 nmol) and DMA (2.7–15.0 nmol). The adsorption isotherms of **2e** into the LP showed Langmuir-type adsorption with binding constants in 2.87×10^6 M^{-1} through the hydrophobic interactions with the dodecyloxo ligand and the core of the LP membrane. The solution was irradiated at 550 nm with gentle stirring under an aerated atmosphere at 25°C. The photoreaction was monitored by the fluorescence coming from DMA at 430 nm under an excitation at 375 nm, since the epidioxy-DMA was nonfluorescent.

From the kinetic analysis, the limiting quantum yield was determined to be 0.73. The reaction was not suppressed by the addition of NaN$_3$ which is known to be a quencher for $^1O_2$. Moreover, the electron transfer from DMA to the ^{1}**2e*** was a favorable exothermic process, since free energy change was calculated to be −0.51 eV by the Rehm-Weller equation. Therefore, it was postulated that the photosensitized oxygenation reaction of DMA with **2e** in the LP occurred through
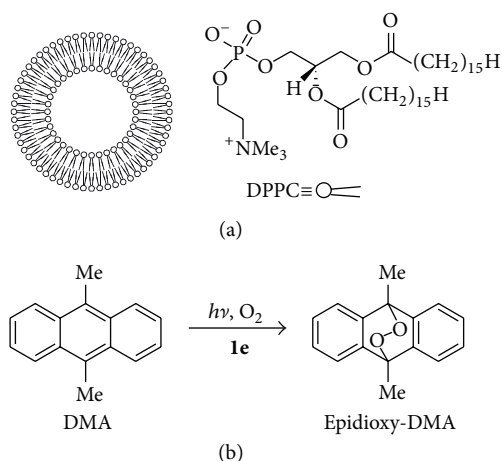
SCHEME 11: (a) Phospholipid liposome which was prepared by DPPC and (b) photosensitized oxidation of DMA with **1e**.

Type I mechanism where photoinduced electron transfer from DMA to the excited singlet state of **1e** (^{1}**1e***) took place to generate **2e**$^{-\bullet}$ and DMA$^{+\bullet}$. The DMA$^{+\bullet}$ reacted with $O_2^{-\bullet}$ which was generated from the reduction of O_2 by **2e**$^{-\bullet}$ to produce epidioxy-DMA.

5. Conclusions

A variety of porphyrins have been applied as the drug for PDT [59]. In general, PDT can damage cancer cells through generation of $^1O_2$ by photosensitized energy transfer (Type II mechanism) [60]. Free base type of porphyrin compounds (e.g., photofrin) has been used as Type II photosensitizer because their protonated species have water solubility and strong absorption in visible region with sufficient triplet energy to produce the excited singlet state of oxygen ($^1O_2^*$; excited energy = 0.98 eV, 1270 nm) [61]. Also the photosensitized damage through generation of ion radicals by photoinduced electron transfer (Type I mechanism) has received much attention because Type I mechanism can operate even under low O_2 concentration in tumor cell. Metalloporphyrins are an attractive candidate because of relatively high electron-accepting power compared with free base porphyrins. Metalloporphyrin complexes have redox properties depending on the interaction between central metal and tetraphenylporphyrinato (tpp) chromophore. Reduction potentials of five-valent P and Sb complexes such as **2b** (−0.50 V versus SCE) [28] and **1b** (−0.51 V) [2] were relatively shifted to positive compared with those of two-valent metal complex such as (tpp)Zn (−1.31 V), (tpp)Ni (−1.18 V), and (tpp)Pb (−1.10 V) [2]. Therefore it is expected that water-soluble P(V) and Sb(V) porphyrins can inactivate cancer cells through both Types I and II mechanisms.
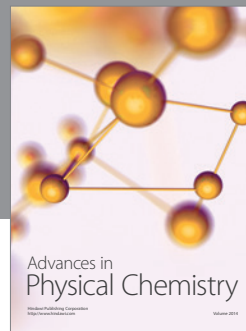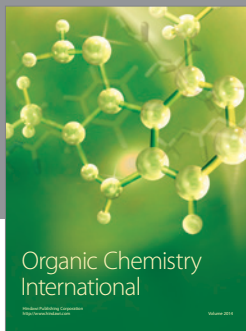
Conflict of Interests

The authors declare that there is no conflict of interests regarding the publication of this paper.

References

[1] R. P. Haugland, *Handbook of Fluorescent Probes and Research Products*, Molecular Probes, Eugene, Ore, USA, 9th edition, 2002.

[2] T. Shiragami, J. Matsumoto, H. Inoue, and M. Yasuda, "Antimony porphyrin complexes as visible-light driven photocatalyst," *Journal of Photochemistry and Photobiology C: Photochemistry Reviews*, vol. 6, no. 4, pp. 227–248, 2005.

[3] E. Alves, M. A. F. Faustino, M. G. P. M. S. Neves, Â. Cunha, H. Nadais, and A. Almeida, "Potential applications of porphyrins in photodynamic inactivation beyond the medical scope," *Journal of Photochemistry and Photobiology C: Photochemistry Reviews*, vol. 22, pp. 34–57, 2015.

[4] L. B. Josefsen and R. W. Boyle, "Unique diagnostic and therapeutic roles of porphyrins and phthalocyanines in photodynamic therapy, imaging and theranostics," *Theranostics*, vol. 2, no. 9, pp. 916–966, 2012.

[5] N. V. Kudinova and T. T. Berezov, "Photodynamic therapy of cancer: search for ideal photosensitizer," *Biochemistry (Moscow) Supplement Series B: Biomedical Chemistry*, vol. 4, no. 1, pp. 95–103, 2010.

[6] E. S. Nyman and P. H. Hynninen, "Research advances in the use of tetrapyrrolic photosensitizers for photodynamic therapy," *Journal of Photochemistry and Photobiology B: Biology*, vol. 73, no. 1-2, pp. 1–28, 2004.

[7] M. Wainwright, "Photodynamic therapy: the development of new photosensitisers," *Anti-Cancer Agents in Medicinal Chemistry*, vol. 8, no. 3, pp. 280–291, 2008.

[8] R. H. Jin, S. Aoki, and K. Shima, "A new route to water soluble porphyrins: phosphonium and ammonium type cationic porphyrins and self-assembly," *Chemical Communications*, no. 16, pp. 1939–1940, 1996.

[9] K. Lang, J. Mosinger, and D. M. Wagnerová, "Photophysical properties of porphyrinoid sensitizers non-covalently bound to host molecules; models for photodynamic therapy," *Coordination Chemistry Reviews*, vol. 248, no. 3-4, pp. 321–350, 2004.

[10] S. Banfi, E. Caruso, L. Buccafurni et al., "Antibacterial activity of tetraaryl-porphyrin photosensitizers: an in vitro study on Gram negative and Gram positive bacteria," *Journal of Photochemistry and Photobiology B: Biology*, vol. 85, no. 1, pp. 28–38, 2006.

[11] I. Batinic-Haberle, I. Spasojevic, H. M. Tse et al., "Design of Mn porphyrins for treating oxidative stress injuries and their redox-based regulation of cellular transcriptional activities," *Amino Acids*, vol. 42, no. 1, pp. 95–113, 2012.

[12] K. Kano, K. Fukuda, H. Wakami, R. Nishiyabu, and R. F. Pasternack, "Factors influencing self-aggregation tendencies of cationic porphyrins in aqueous solution," *Journal of the American Chemical Society*, vol. 122, no. 31, pp. 7494–7502, 2000.

[13] P. Kubát, K. Lang, P. Anzenbacher Jr., K. Jursíková, V. Král, and B. Ehrenberg, "Interaction of novel cationic meso-tetraphenylporphyrins in the ground and excited states with DNA and nucleotides," *Journal of the Chemical Society, Perkin Transactions 1*, no. 6, pp. 933–941, 2000.

[14] Y. Cao, A. F. Gill, and D. W. Dixon, "Synthesis and characterization of a water-soluble porphyrin with a cyclic sulfone," *Tetrahedron Letters*, vol. 50, no. 30, pp. 4358–4360, 2009.

[15] J. M. Dąbrowski, M. M. Pereira, L. G. Arnaut et al., "Synthesis, photophysical studies and anticancer activity of a new halogenated water-soluble porphyrin," *Photochemistry and Photobiology*, vol. 83, no. 4, pp. 897–903, 2007.

[16] X. Zhang, K. Sasaki, and Y. Kuroda, "Characterization of magnesium porphyrins and aggregation of porphyrins in organic solvent," *Bulletin of the Chemical Society of Japan*, vol. 80, no. 3, pp. 536–542, 2007.

[17] R. H. Jin, S. Aoki, and K. Shima, "Phosphoniumyl cationic porphyrins Self-aggregation origin from π-π and cation-π interactions," *Journal of the Chemical Society—Faraday Transactions*, vol. 93, no. 22, pp. 3945–3953, 1997.

[18] H. Imai, H. Munakata, Y. Uemori, and N. Sakura, "Chiral recognition of amino acids and dipeptides by a water-soluble zinc porphyrin," *Inorganic Chemistry*, vol. 43, no. 4, pp. 1211–1213, 2004.

[19] J. Matsumoto, T. Shiragami, and M. Yasuda, "Water-soluble porphyrin easily derived from tetraphenylporphyrin: alkyloxo(methoxo)porphyrinatoantimony bromides," *Chemistry Letters*, vol. 37, no. 8, pp. 886–887, 2008.

[20] J. Matsumoto, S.-I. Tanimura, T. Shiragami, and M. Yasuda, "Water-solubilization of alkyloxo(methoxo)porphyrinatoantimony bromides," *Physical Chemistry Chemical Physics*, vol. 11, no. 42, pp. 9766–9771, 2009.

[21] M. Yasuda, T. Nakahara, T. Matsumoto et al., "Visible light-assisted sterilization activity of water-soluble antimonyporphyrin toward *Saccharomyces cerevisiae*," *Journal of Photochemistry and Photobiology A: Chemistry*, vol. 205, no. 2-3, pp. 210–214, 2009.

[22] J. Matsumoto, S.-I. Tanimura, T. Shiragami, and M. Yasuda, "Concentration-dependent aggregation of water-soluble phosphorus porphyrin in an aqueous solution," *Journal of Porphyrins and Phthalocyanines*, vol. 16, no. 2, pp. 210–217, 2012.

[23] J. Matsumoto, T. Shinbara, S.-I. Tanimura et al., "Water-soluble phosphorus porphyrins with high activity for visible light-assisted inactivation of *Saccharomyces cerevisiae*," *Journal of Photochemistry and Photobiology A: Chemistry*, vol. 218, no. 1, pp. 178–184, 2011.

[24] J. Matsumoto, T. Kubo, T. Shinbara et al., "Spectroscopic analysis of the interaction of human serum albumin with tricationic phosphorus porphyrins bearing axial pyridinio groups," *Bulletin of the Chemical Society of Japan*, vol. 86, no. 11, pp. 1240–1247, 2013.

[25] J. Matsumoto, T. Beppu, T. Shiragami, and M. Yasuda, "Mechanistic analysis of the fluorescence quenching of dodecyloxo(methoxo) tetraphenylporphyrinatoantimony by 9,10-dimethylanthracene in an artificial membrane constructed by a phospholipid liposome," *Journal of Photochemistry and Photobiology A: Chemistry*, vol. 249, pp. 47–52, 2012.

[26] K. Kalyanasundaram, "Photochemistry of water-soluble porphyrins: comparative study of isomeric tetrapyridyl- and tetrakis(*N*-methylpyridiniumyl)porphyrins," *Inorganic Chemistry*, vol. 23, no. 16, pp. 2453–2459, 1984.

[27] M. Yasuda, T. Shiragami, and J. Matsumoto, "Water-soluble porphyrin and process for production thereof," JP Patent no. JP20090233246, 2009.

[28] K. Hirakawa, N. Fukunaga, Y. Nishimura, T. Arai, and S. Okazaki, "Photosensitized protein damage by dimethoxyphosphorus(V) tetraphenylporphyrin," *Bioorganic and Medicinal Chemistry Letters*, vol. 23, no. 9, pp. 2704–2707, 2013.

[29] R. Marczak, V. Sgobba, W. Kutner, S. Gadde, F. D'Souza, and D. M. Guldi, "Langmuir-blodgett films of a cationic zinc porphyrin-Imidazole-functionalized fullerene dyad: formation and photoelectrochemical studies," *Langmuir*, vol. 23, no. 4, pp. 1917–1923, 2007.

[30] M. Sirish, V. A. Chertkov, and H.-J. Schneider, "Porphyrin-based peptide receptors: syntheses and NMR analysis," *Chemistry—A European Journal*, vol. 8, no. 5, p. 1181, 2002.

[31] O. Yaffe, E. Korin, and A. Bettelheim, "Interaction of Fe(III) tetrakis(4-*N*-methylpyridinium)porphyrin with sodium dodecyl sulfate at submicellar concentrations," *Langmuir*, vol. 24, no. 20, pp. 11514–11517, 2008.

[32] Y. H. Kim, S. D. Jung, M. H. Lee et al., "Photoinduced reduction of manganese(III) *meso*-tetrakis(1-methylpyridinium-4-yl)porphyrin at AT and GC base pairs," *The Journal of Physical Chemistry B*, vol. 117, no. 33, pp. 9585–9590, 2013.

[33] R. F. Pasternack, S. Ewen, A. Rao et al., "Interactions of copper(II) porphyrins with DNA," *Inorganica Chimica Acta*, vol. 317, no. 1-2, pp. 59–71, 2001.

[34] J. S. Trommel and L. G. Marzilli, "Synthesis and DNA binding of novel water-soluble cationic methylcobalt porphyrins," *Inorganic Chemistry*, vol. 40, no. 17, pp. 4374–4383, 2001.

[35] M. Haeubl, L. M. Reith, B. Gruber et al., "DNA interactions and photocatalytic strand cleavage by artificial nucleases based on water-soluble gold(III) porphyrins," *Journal of Biological Inorganic Chemistry*, vol. 14, no. 7, pp. 1037–1052, 2009.

[36] S. Naveenraj and S. Anandan, "Binding of serum albumins with bioactive substances—nanoparticles to drugs," *Journal of Photochemistry and Photobiology C: Photochemistry Reviews*, vol. 14, no. 1, pp. 53–71, 2013.

[37] G. Sudlow, D. J. Birkett, and D. N. Wade, "Further characterization of specific drug binding sites on human serum albumin," *Molecular Pharmacology*, vol. 12, no. 6, pp. 1052–1061, 1976.

[38] J. R. Lakowicz, *Principles of Fluorescence Spectroscopy*, Springer, New York, NY, USA, 3rd edition, 2006.

[39] S. S. Wong, T. E. Malone, and T. K. Lee, "Use of concanavalin a as a topographical probe for protein-protein interaction application to lactose synthase," *Biochimica et Biophysica Acta*, vol. 745, no. 1, pp. 90–96, 1983.

[40] K. D. Hardman and C. F. Ainsworth, "Structure of the concanavalin A-methyl α-D-mannopyranoside complex at 6-Å resolution," *Biochemistry*, vol. 15, no. 5, pp. 1120–1128, 1976.

[41] S. J. Harrop, J. R. Helliwell, T. C. M. Wan, A. J. Kalb, L. Tong, and J. Yariv, "Structure solution of a cubic crystal of concanavalin A complexed with methyl α-D-glucopyranoside," *Acta Crystallographica Section D: Biological Crystallography*, vol. 52, no. 1, pp. 143–155, 1996.

[42] K. Hirakawa, T. Hirano, Y. Nishimura, T. Arai, and Y. Nosaka, "Control of singlet oxygen generation photosensitized by meso-anthrylporphyrin through interaction with DNA," *Photochemistry and Photobiology*, vol. 87, no. 4, pp. 833–839, 2011.

[43] K. Hirakawa, M. Harada, S. Okazaki, and Y. Nosaka, "Controlled generation of singlet oxygen by a water-soluble meso-pyrenylporphyrin photosensitizer through interaction with DNA," *Chemical Communications*, vol. 48, no. 39, pp. 4770–4772, 2012.

[44] S. Tada-Oikawa, J. Hirayama, K. Hirakawa, and S. Kawanishi, "DNA damage and apoptosis induced by photosensitization of 5,10,15,20-tetrakis (*N*-methyl-4-pyridyl)-21*H*,23*H*-porphyrin *via* singlet oxygen generation," *Photochemistry and Photobiology*, vol. 85, no. 6, pp. 1391–1399, 2009.

[45] Y. Fueda, M. Hashimoto, K. Nobuhara et al., "Visible-light bactericidal effect of silica gel-supported porphyrinatoantimony(V) catalyst on *Legionella* species occurring in the living environmental fields," *Biocontrol Science*, vol. 10, no. 1-2, pp. 55–60, 2005.

[46] K. Hirakawa, S. Kawanishi, J. Matsumoto, T. Shiragami, and M. Yasuda, "Guanine-specific DNA damage photosensitized by the dihydroxo(tetraphenylporphyrinato)antimony(V) complex," *Journal of Photochemistry and Photobiology B: Biology*, vol. 82, no. 1, pp. 37–44, 2006.

[47] K. Hirakawa, M. Yoshida, S. Oikawa, and S. Kawanishi, "Base oxidation at 5′ site of GG sequence in double-stranded DNA induced by UVA in the presence of xanthone analogues: relationship between the DNA-damaging abilities of photosensitizers and their HOMO energies," *Photochemistry and Photobiology*, vol. 77, no. 4, pp. 349–355, 2003.

[48] F. D. Lewis and Y. Wu, "Dynamics of superexchange photoinduced electron transfer in duplex DNA," *Journal of Photochemistry and Photobiology C: Photochemistry Reviews*, vol. 2, no. 1, pp. 1–16, 2001.

[49] H. Sugiyama and I. Saito, "Theoretical studies of GG-specific photocleavage of DNA via electron transfer: significant lowering of ionization potential and 5′-localization of HOMO of stacked GG bases in B-form DNA," *Journal of the American Chemical Society*, vol. 118, no. 30, pp. 7063–7068, 1996.

[50] Y. Yoshioka, Y. Kitagawa, Y. Takano, K. Yamaguchi, T. Nakamura, and I. Saito, "Experimental and theoretical studies on the selectivity of GGG triplets toward one-electron oxidation in B-form DNA," *Journal of the American Chemical Society*, vol. 121, no. 38, pp. 8712–8719, 1999.

[51] K. Hirakawa, S. Kawanishi, T. Hirano, and H. Segawa, "Guanine-specific DNA oxidation photosensitized by the tetraphenylporphyrin phosphorus(V) complex via singlet oxygen generation and electron transfer," *Journal of Photochemistry and Photobiology B: Biology*, vol. 87, no. 3, pp. 209–217, 2007.

[52] K. Hirakawa, K. Azumi, Y. Nishimura, T. Arai, Y. Nosaka, and S. Okazaki, "Photosensitized damage of protein by fluorinated diethoxyphosphorus(V) porphyrin," *Journal of Porphyrins and Phthalocyanines*, vol. 17, no. 1-2, pp. 56–62, 2013.

[53] H. Yokoi, T. Shiragami, J. Hirose et al., "Bactericidal effect of a silica gel-supported porphyrinatoantimony(V) complex under visible light irradiation," *World Journal of Microbiology and Biotechnology*, vol. 19, no. 6, pp. 559–563, 2003.

[54] Y. Fueda, H. Suzuki, Y. Komiya et al., "Bactericidal effect of silica gel-supported porphyrinatophosphorus(V) catalysts on *Escherichia coli* under visible-light irradiation," *Bulletin of the Chemical Society of Japan*, vol. 79, no. 9, pp. 1420–1425, 2006.

[55] C. Tanielian and C. Wolff, "Porphyrin-sensitized generation of singlet molecular oxygen: comparison of steady-state and time-resolved methods," *Journal of Physical Chemistry*, vol. 99, no. 24, pp. 9825–9830, 1995.

[56] A. Gomes, E. Fernandes, and J. L. F. C. Lima, "Fluorescence probes used for detection of reactive oxygen species," *Journal of Biochemical and Biophysical Methods*, vol. 65, no. 2-3, pp. 45–80, 2005.

[57] H. Kotani, K. Ohkubo, and S. Fukuzumi, "Photocatalytic oxygenation of anthracenes and olefins with dioxygen via selective radical coupling using 9-mesityl-10-methylacridinium ion as an effective electron-transfer photocatalyst," *Journal of the American Chemical Society*, vol. 126, no. 49, pp. 15999–16006, 2004.

[58] A. D. Bangham, M. M. Standish, and J. C. Watkins, "Diffusion of univalent ions across the lamellae of swollen phospholipids," *Journal of Molecular Biology*, vol. 13, no. 1, pp. 238–252, 1965.

[59] M. R. Hamblin and T. Hasan, "Photodynamic therapy: a new antimicrobial approach to infectious disease?" *Photochemical and Photobiological Sciences*, vol. 3, no. 5, pp. 436–450, 2004.

[60] I. J. MacDonald and T. J. Dougherty, "Basic principles of pho-
todynamic therapy," *Journal of Porphyrins and Phthalocyanines*,
vol. 5, no. 2, pp. 105–129, 2001.

[61] R. K. Pandey and G. Zheng, "Porphyrins as photosensitizers
in photodynamic therapy," in *The Porphyrin Handbook*, K.
M. Kadish, K. M. Smith, and R. Guilluy, Eds., pp. 157–230,
Academic Press, San Diego, Calif, USA, 2000.